RSC Advances

PAPER

View Article Online
View Journal | View Issue

Cite this: *RSC Adv.*, 2015, **5**, 22980

Energy decomposition analysis of *gauche* preference in 2-haloethanol, 2-haloethylamine (halogen = F, Cl), their protonated forms and *anti* preference in 1-chloro-2-fluoroethane†

Marija Baranac-Stojanović,*[a] Jovana Aleksić[b] and Milovan Stojanović[b]

2-Haloethanol and 2-haloethylamine (halogen = F, Cl) prefer *gauche* conformation. This preference is significantly increased upon protonation. Commonly used explanations are based on intramolecular hydrogen bonding and hyperconjugation. 1,2-Difluoroethane prefers *gauche* conformation, too, while gaseous 1-chloro-2-fluoroethane is more stable as the *anti* conformer. The origin of these conformational preferences has been investigated by a quantitative partitioning of the *gauche*/*anti* energy difference into contributions from electrostatic, orbital, dispersion and Pauli interactions, and structural changes accompanying the rotation. The results show that, with two exceptions, the most important contributor to the *gauche* preference is electrostatic attraction, which is larger in *gauche* forms relative to the *anti* ones. Next come orbital interactions, while dispersion forces provide the smallest stabilizing energy. These energy components override destabilizing Pauli interactions and energetically costly structural changes. All *gauche* preferences also benefit from stereoelectronic effects, except in protonated 2-chloroethanol which, instead, shows a significant Cl lone pair → O–H antibond mixing, associated with hydrogen bonding. The increase in the Pauli repulsion upon *anti* to *gauche* isomerization is more pronounced for fluorine than for chlorine derivatives. Thus, the smaller *gauche* effect in chloro-compounds and the *anti* preference in 1-chloro-2-fluoroethane have their origin in the decrease in electrostatic and orbital stabilizing interactions, a drop in the former being more pronounced.

Received 20th January 2015
Accepted 25th February 2015

DOI: 10.1039/c5ra01164g

www.rsc.org/advances

Introduction

Fluorine is the most electronegative atom in the periodic table and thus the C–F bond is the most polar bond in organic chemistry.[1] Therefore, the observation that 1,2-difluoroethane (DFE) prefers *gauche* conformation over the *anti* by 0.5–1 kcal mol^{-1} (ref. 2 and 3) is surprising, taking into account the expected strong repulsive interaction between the two C–F bond dipoles in the *gauche* form. This *gauche* preference, also termed as *gauche* effect,[4] has been rationalized by the bent bond model of Wiberg *et al.*[5] according to which electronegative fluorine atoms cause C–C bond bending in both *anti* and *gauche* forms, but leading to poorer orbital overlap in the former. Another, more widely used explanation is based on hyperconjugation. Thus, the two vicinal $\sigma_{C-H} \rightarrow \sigma^*_{C-F}$ hyperconjugative interactions are involved in the stabilization of the *gauche* conformer.[3c,d,6] Recently, we proposed that *gauche*-DFE also benefits from more favourable electrostatic interactions, that is, this type of interactions should be considered as an all-charge phenomenon rather than partial interaction between pairs of bonds.[7] This finding was in accord with an earlier explanation of the *gauche* effect in various compounds as a prevailing nucleus–electron attraction over nucleus–nucleus and electron–electron repulsion.[4]

The fluorine *gauche* effect was found experimentally and/or theoretically in various other compounds having an electronegative substituent in β-position to the fluorine atom, such as *O*-β-fluoroethyl esters,[8] *N*-β-fluoroethylamides,[9] 1-fluoro-2-nitroethane,[10] 1-azido-2-fluoroethane,[10] 1-fluoro-2-iso(thio) cyanatoethane,[10] 2-fluoroimines,[11] 2-fluoroethanol[12] and 2-fluoroethylamine.[12e,13] Its origin is commonly ascribed to stereoelectronic effects, that is, the stabilizing hyperconjugative interactions wherein σ^*_{C-F} and σ^*_{C-X} orbitals (X = electronegative atom in β-position to F) act as acceptors of electron density donated from antiperiplanar σ_{C-H} bonds in *gauche* forms. Electrostatic attraction between fluorine and an electropositive atom contained in a β-substituent may add additional stabilization.[10] Although, the conformational behaviour of 2-fluoroethanol (FE) has been ascribed to intramolecular hydrogen

[a]*Faculty of Chemistry, University of Belgrade, Studentski trg 12-16, P. O. Box 158, 11000 Belgrade, Serbia. E-mail: mbaranac@chem.bg.ac.rs*

[b]*Center for Chemistry ICTM, University of Belgrade, P. O. Box 473, 11000 Belgrade, Serbia*

† Electronic supplementary information (ESI) available: Optimized structural parameters, comparison of LMOEDA and NBOEDA results, absolute energies and *x*, *y*, *z* coordinates of the studied molecules. See DOI: 10.1039/c5ra01164g

bonding interactions[12a] rather than stereoelectronic effects,[12b,e] this explanation was questioned[12h] based on the facts that organic fluorine is poor hydrogen bond acceptor.[14] In particular, fluorine atom hardly accepts intramolecular five-membered F···H–O hydrogen bond due to geometric restrictions, which do not allow sufficiently close contact between F and H atoms.[12h,15] Instead, the *gauche* prevalence in FE may stem from an electrostatic attraction between antiparallel OH and CF bond dipoles[12d] and stronger hyperconjugative interactions.[12f] Although, a repulsion between the lone pair electrons on oxygen and fluorine atoms could also turn the hydroxyl hydrogen atom toward the fluorine.[12c] The larger stability of *gauche* forms in 2-fluoroethylamine (FEA) has also been attributed to the formation of intramolecular hydrogen bonds,[12e,13b] seen as an electrostatic attractive interaction between the N–H and C–F bond dipoles, rather than covalent bonding.[13a]

Protonation of FEA increases *gauche* preference from 1.0 kcal mol^{-1} in neutral amine to 5.8 kcal mol^{-1} in 2-fluoroethylammonium ion (FEAH), while protonation of FE results in *gauche* preference of 7.2 kcal mol^{-1} relative to 2.0 kcal mol^{-1} for the alcohol.[12e] Both stereoelectronic effects and intramolecular hydrogen bonding interactions were invoked to explain the calculated large stability of *gauche* conformers relative to their *anti* counterparts.[12e] However, X-ray structure analysis of 2-fluoroethylammonium chloride revealed no intramolecular F···H–N hydrogen bonding interaction.[12e] Later theoretical work showed that the strength of hyperconjugative interactions is similar in *gauche*-FEA and its protonated structure, and the larger stabilization of *gauche*-FEAH *vs. anti*-FEAH as compared to that of *gauche*-FEA *vs. anti*-FEA was attributed to strong intramolecular F···H–N hydrogen bonding in the protonated *gauche* form.[13c] An additional explanation is based on electrostatic interactions.[10] The fluorine *gauche* effect extends to the related (a)cyclic systems containing positively charged nitrogen atom and is ascribed to the strong through space charge–dipole or dipole–dipole ($^{+}$N–H and C–F) attractive interaction, the strength of which compares with that of a reasonably strong hydrogen bond.[16]

Hence, introduction of fluorine atom β to an electronegative substituent has important consequences on conformational behaviour and has emerged as a powerful tool in synthetic organic chemistry.[17]

The replacement of fluorine with chlorine atom in DFE results in a loss of *gauche* preference in 1-chloro-2-fluoroethane (CFE) in the gas phase.[3a,12d,18] The same replacement in FE and FEA retains the *gauche* preference in 2-chloroethanol (CE)[12d,f,g,19] and 2-chloroethylamine (CEA),[20] but decreases the energy differences between *gauche* and *anti* forms relative to those for fluorine compounds. In both CE and CEA, the dominance of *gauche* conformers has been attributed to stabilizing intramolecular hydrogen bonding interactions[19a] usually described as an electrostatic attraction between antiparallel C–Cl and O(N)–H bond dipoles.[12d,f,19b,c,20] The operation of hyperconjugative interactions was invoked, too.[12f] The enhanced stability of the *anti*-CFE relative to the *gauche*-CFE was rationalized as a combination of electrostatic repulsion between the C–F and C–Cl bond dipoles and a weaker hyperconjugative preference for *gauche* form.[3a] A smaller tendency of chlorinated compounds for *gauche* conformation compared with fluoro derivatives could be anticipated on the basis of chlorine's larger size (van der Waals radii of F and Cl atoms are 1.47 Å and 1.75 Å, respectively),[21] thus introducing larger steric repulsion in *gauche* forms. The electrostatic repulsion between bond dipoles in *gauche* forms is expected to be smaller. Though, other factors, such as hyperconjugation, should play a role, as well. Unlike fluoro derivatives, chlorine-containing molecules have been less studied with respect to the origin of their conformational preferences.

Understanding the factors governing conformational behaviour is crucial to address various questions in organic chemistry and biochemistry, since molecular properties, reactivity and interactions with other molecules are influenced by their conformation. The purpose of this study is to quantitatively decompose the energy difference between *gauche* and *anti* conformers of FE, CE, FEA, CEA and their protonated forms into contributions from electrostatic, orbital and dispersion interactions, Pauli repulsion and energy required for structural changes and thus to get a further insight into the origin of *gauche* effect in these molecules. One aim is also to explain the weaker tendency for *gauche* conformations in the chloro derivatives. For the latter to be done, CFE and DFE were also included in the study. The results would deepen our knowledge about the origin of conformational behaviour of the mentioned and related molecules, the importance of which is also reflected in the increasing application of fluorine compounds in organic and medicinal chemistry.[11,16b,17] To the best of our knowledge, no such an attempt has been made, though quantifications of some of the interactions considered to be involved have been done. These include hyperconjugative interactions and intramolecular hydrogen bonding/antiparallel dipoles attraction, often estimated on the basis of the natural bond orbital (NBO) analysis[10,12d,f,h,13c] or from the relative energies of corresponding conformers.[12b,e,19a]

Computational details

Various conformers of studied compounds were fully optimized at the MP2/6-311++G** level[22] using the Gaussian 09 program package.[23] They were characterized as energy minima by the absence of imaginary frequencies. In the following conformational energy analysis, done at the same level of theory, overall molecules have been built from the two radicals $XH_2C^{\bullet}$ (X = F, Cl) and $^{\bullet}CH_2Y$ (Y = F, OH, $^{+}OH_2$, NH_2, $^{+}NH_3$), taken with opposite spins (α and β superscripts in Scheme 1) so that they can form a bond.

Total binding energy ΔE between them consists of two major parts (eqn (1)):

$$\Delta E = \Delta E_{\text{prep}} + \Delta E_{\text{int}} \quad (1)$$

$$XH_2C^{\alpha} + {}^{\beta}CH_2Y \rightarrow XH_2C{-}CH_2Y$$

Scheme 1

In the equation, the preparation energy ΔE_{prep} represents the amount of energy required to deform two isolated radicals ($XH_2C^{\bullet}$ and $^{\bullet}CH_2Y$) from their equilibrium geometry to the geometry they adopt in the final molecules. The interaction energy ΔE_{int} is the energy change occurring when prepared (deformed) fragments $XH_2C^{\bullet}$ and $^{\bullet}CH_2Y$ combine to form the molecule. The latter energy term can be further decomposed into five components (eqn (2)) by using the localized molecular orbital energy decomposition analysis (LMOEDA),[24] implemented in the Gamess program package.[25]

$$\Delta E_{int} = \Delta E_{elstat} + \Delta E_{ex} + \Delta E_{rep} + \Delta E_{pol} + \Delta E_{disp} \quad (2)$$

The electrostatic energy ΔE_{elstat} corresponds to nucleus–nucleus and electron–electron repulsion, and nucleus–electron attraction between the two prepared radical fragments that adopt their positions in the final molecule, and is usually stabilizing (attractive). The exchange energy ΔE_{ex} refers to the quantum mechanical exchange between the same-spin electrons and is simultaneously counteracted by the repulsion energy ΔE_{rep}. Taken together, they form the exchange repulsion[26] or Pauli repulsion[27] of other EDA schemes, which is a destabilizing interaction, also referred to, herein, as the steric repulsion. This type of repulsion is caused by the fact that two electrons with the same spin cannot occupy the same region in space. The polarization energy ΔE_{pol} is an orbital relaxation energy which comes from a change in orbital shapes upon binding and also includes empty-occupied orbital mixing within one fragment due to the presence of another (polarization) and between two fragments (charge transfer). The dispersion energy term ΔE_{disp} at the MP2 level comes from electron correlation correction to the Hartree–Fock interaction energy. The energy change that follows *anti* → *gauche* rotation is calculated as a difference between total binding energies of *gauche* and *anti* conformers, where the change in the ΔE_{prep} reflects gain or loss in energy due to the structural changes that accompany the conformational isomerization, whereas the change in the ΔE_{int} is associated with the change in the nature of chemical bonding. Such an analysis of the interaction energy between two or more fragments constituting a molecule has been applied before to study the rotational barrier in ethane[24,28] and in group 13-elements (E = B – Tl),[29] distortion to the *trans*-bent geometry in heavier ethylene homologues,[30] the isomerization energy of heterocyclic[31] and polycyclic[32] compounds, the strength of conjugation and hyperconjugation,[33] and the nature of covalent bonds.[34]

Energies of hyperconjugative interactions were calculated by using the natural bond orbital (NBO) analysis (NBO version 6.0 (ref. 35) linked to G09 was employed).

Results and discussion

1,2-Difluoroethane and 1-chloro-2-fluoroethane

The MP2/6-311++G** optimized bond lengths, bond angles and torsional angles for *anti* and *gauche* conformers of 1,2-difluoroethane (DFE) and 1-chloro-2-fluoroethane (CFE) are given in Tables S1 and S2 in the ESI.† They are very close to the experimental values obtained from infrared[36] and microwave[37] spectroscopy, and electron diffraction.[18a] In the case of DFE, *gauche* conformer is more stable than *anti* by $\Delta E = -0.77$ kcal mol^{-1} (*a*-DFE → *g*-DFE in Fig. 1 and Table 1). This is in accord with previous experimental and theoretical results.[2,3] By contrast, CFE prefers *anti* conformation by $\Delta E = 0.52$ kcal mol^{-1} (*a*-CFE → *g*-CFE in Fig. 1 and Table 1), which also compares with previous estimates in the gas phase.[3a,12d,18] Table 1 lists the energy decomposition results for *anti* and *gauche* conformers of DFE and CFE (*a*-DFE, *g*-DFE, *a*-CFE and *g*-CFE) and for the *anti* → *gauche* rotation of both molecules (*a*-DFE → *g*-DFE and *a*-CFE → *g*-CFE).

Our MP2 results for DFE agree with previously reported B3LYP/6-311+G** results[7] that the conformational preference in DFE comes from the more favourable interaction energy term $\Delta E_{int} = -0.95$ kcal mol^{-1}, while the preparation energy slightly disfavours the *gauche* conformation. Somewhat unexpectedly, data in Table 1, like those in the previous publication,[7] show that *g*-DFE is stabilized not only by more favourable orbital interactions ($\Delta E_{pol} = -4.53$ kcal mol^{-1}), but also by more attractive electrostatic interactions ($\Delta E_{elstat} = -3.38$ kcal mol^{-1}). This finding points to the conclusion that electrostatic interactions should be considered as an all-charge phenomenon, rather than partial interactions between pairs of bonds. Dispersion energy $\Delta E_{disp} = -0.61$ kcal mol^{-1}, too, slightly favours *gauche* conformation and the only destabilizing interaction in the ΔE_{int} energy part is steric repulsion coming from Pauli interactions.

In CFE, *gauche* conformer is disfavoured by both $\Delta E_{int} = 0.34$ kcal mol^{-1} and $\Delta E_{prep} = 0.18$ kcal mol^{-1}. It is of interest to analyze the origin of destabilizing ΔE_{int} compared to the stabilizing ΔE_{int} in DFE. An intuitive explanation for the reversal of conformational preferences in DFE and CFE would be a stronger steric repulsion between the more voluminous chlorine and the *gauche* oriented fluorine atom in *g*-CFE than between the two fluorine atoms in *g*-DFE. As Table 1 shows, the steric repulsion indeed increases when *a*-CFE rotates to *g*-CFE ($\Delta E_{ex+rep} = 3.66$ kcal mol^{-1}), but this energy rise is smaller than that for DFE ($\Delta E_{ex+rep} = 7.57$ kcal mol^{-1}). It should be noted that this steric repulsion reflects the all-electron repulsive interactions, not just those between halogen atoms which are by 0.06 Å closer to each other in DFE than their van der Waals radii would allow, and by 0.10 Å in CFE. Thus, the steric repulsion cannot account for the reversal of conformational preference in CFE compared to that in DFE. The data in Table 1 show that the nature of stabilizing interactions is practically the same in two conformers of both DFE and CFE: ΔE_{pol} is the largest attractive component contributing about 47% of all attractive forces, next comes ΔE_{elstat} (about 45%), while ΔE_{disp} contributes the smallest stabilization (about 8%). However, their magnitude differ. Upon *a* → *g* rotation, these three interactions provide much more stabilization in the case of DFE, which overcomes the destabilizing steric repulsion and leads to the overall negative interaction energy (stabilization of *gauche* conformer). In the case of CFE, the change in the magnitude of stabilizing interactions upon *a* → *g* isomerization is not large enough to overcome the increase in the steric repulsion. Thus, it is a drop in electrostatic, orbital and dispersion interactions, following the

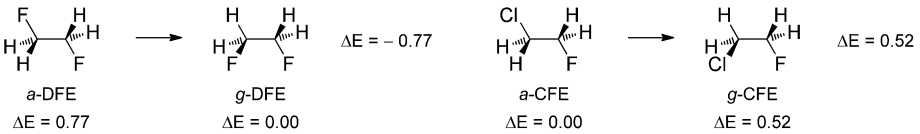

Fig. 1 Energy minimum conformations of 1,2-difluoroethane (DFE) and 2-chloro-1-fluoroethane (CFE), their relative electronic energies (kcal mol^{-1}) and energy changes occurring upon *anti* → *gauche* rotation.

isomerization, which is responsible for the *anti* preference in isolated CFE. The energy gain due to structural changes occurring upon isomerization is the same in both molecules (ΔE_{prep} in Table 1).

Since the LMOEDA does not allow separation of charge transfer interactions from other orbital interactions, vicinal hyperconjugative interactions, often invoked to explain *gauche* preferences,[3c,d,6,10] were estimated by using the NBO analysis, at the HF/6-311++G** level. Within the NBO framework, the stabilizing energy gained from delocalization of electron density from filled orbitals to empty antibonding orbitals can be calculated by a second-order perturbation approach (referred to as $E(2)$ energies) or by deletion of the corresponding off-diagonal elements of the Fock matrix in the NBO basis and recalculating the energy (referred to as E(del) energies).[38] We used both approaches for the calculation of all vicinal hyperconjugative interactions (*synclinal* and *anti*) between XCH_2 and CH_2Y fragments. For $E(2)$ energies, this corresponds to the sum of all vicinal interactions. For E(del) energies, we set to zero all Fock matrix elements corresponding to delocalizing interactions from C–H and C–X orbitals on one fragment into the antibonding C–H and C–Y orbitals on another fragment, and *vice versa* (deletion type 3 in NBO Manual, p. B-17).[38c] The calculated values correlate well with each other for all molecules considered, as has also been shown for other systems.[6b,38,39] Data for DFE and CFE are given in Table 2 as $E(2)_{synclinal/anti}$ and $E(del)_{synclinal/anti}$, respectively, and for other compounds in tables that will be discussed later. A change in hyperconjugative interaction energy occurring upon *anti* → *gauche* isomerization is denoted as $E(2)_{synclinal/anti}$ $a \rightarrow g$ and $E(del)_{synclinal/anti}$ $a \rightarrow g$ in all tables considering these interactions. The more positive value means stronger interaction.

The results from the second-order perturbation approach (individual $E(2)$ values) showed that *anti* hyperconjugative interactions account for the majority of these charge transfer interactions and they are the most affected by rotation. The *synclinal* interactions change little upon rotation for all studied molecules (less than 0.5 kcal mol^{-1}), whereas changes in *anti* interactions can reach values of 6.4 kcal mol^{-1}. For these reasons, only individual *anti* hyperconjugative interactions obtained from the second-order perturbation approach are shown in tables, where total $E(2)_{anti}$ values represent the sum of the six interactions for corresponding conformers, and total $E(2)_{anti}$ $a \rightarrow g$ values show their change upon the rotation.

The results in Table 2 show that *gauche* conformers of both DFE and CFE are more stabilized by hyperconjugation than their *anti* counterparts, so that stereoelectronic effects favour *gauche* forms. The most important contributions come from C–H → C–F* and C–H → C–Cl* delocalizations. The latter one is more stabilizing, which is in accord with the stronger electron-accepting ability of the C–Cl* antibond *vs.* C–F* antibond, due to its lower energy.[6b] There is an increase in the hyperconjugative stabilization in *g*-CFE relative to *g*-DFE. This increase originates mainly from the larger C–H → C–Cl* and C–Cl → C–H* delocalizations ($E(2)_{C-H \rightarrow C-Cl^*} = 6.82$ kcal mol^{-1} *vs.* $E(2)_{C-H \rightarrow C-F^*} = 5.81$ kcal mol^{-1}, $E(2)_{C-Cl \rightarrow C-H^*} = 1.91$ kcal mol^{-1} *vs.* $E(2)_{C-F \rightarrow C-H^*} = 0.85$ kcal mol^{-1}), showing that the C–Cl bond is also a better electron-donor due to its higher energy relative to energy of the C–F bond orbital. The *anti* conformer of CFE is also better stabilized by hyperconjugation than is *anti* conformer of DFE, mostly because of an increased C–Cl → C–F* interaction (3.76 kcal mol^{-1}) in *a*-CFE compared to the C–F → C–F* one in *a*-DFE (1.80 kcal mol^{-1}), though other interactions contribute, as well. The increase in hyperconjugative stabilization in *a*-CFE *vs.* *a*-DFE exceeds the increase in hyperconjugative stabilization in *g*-CFE *vs.* *g*-DFE. As a result, the *anti* → *gauche* conformational change benefits less from hyperconjugation, both total and *anti*, in CFE compared to DFE (Table 2). Overall, both hyperconjugative and all orbital interactions (ΔE_{pol} in Table 1) contribute less stabilizing energy

Table 1 Contribution of various energy terms to the total binding interactions between two $FH_2C^{\bullet}$ and $^{\bullet}CH_2Y$ radicals and to the *anti* → *gauche* energy change in 1,2-difluoroethane (DFE, Y = F) and 1-chloro-2-fluoroethane (CFE, Y = Cl).[a] Values are in kcal mol^{-1}

Conformation	ΔE_{elstat}	ΔE_{ex+rep}	ΔE_{pol}	ΔE_{disp}	ΔE_{int}	ΔE_{prep}	ΔE
a-DFE	−148.82	221.67	−155.48	−25.50	−108.13	10.31	−97.82
g-DFE	−152.20	229.24	−160.01	−26.11	−109.08	10.50	−98.58
a-DFE → *g*-DFE	−3.38	7.57	−4.53	−0.61	−0.95	0.18	−0.77
a-CFE	−149.20	225.17	−156.91	−29.12	−110.06	12.05	−98.01
g-CFE	−150.02	228.83	−159.04	−29.49	−109.72	12.24	−97.48
a-CFE → *g*-CFE	−0.82	3.66	−2.13	−0.37	0.34	0.18	0.52

[a] ΔE_{elstat} = electrostatic energy, ΔE_{ex+rep} = exchange repulsion energy, ΔE_{pol} = polarization energy, ΔE_{disp} = dispersion energy, ΔE_{int} = interaction energy, ΔE_{prep} = preparation energy, ΔE = total binding energy.

Table 2 Energies (in kcal mol^{-1}) of vicinal hyperconjugative interactions in 1,2-difluoroethane (DFE, Y = F) and 1,2-dichoroethane (CFE, Y = Cl) estimated from the second-order perturbative approach, $E(2)$ values, and deletion of the corresponding Fock matrix elements in the NBO basis, E(del). Calculated at the HF/6-311++G** level

	a-DFE	*g*-DFE	*a*-CFE	*g*-CFE
Vicinal hyperconjugation				
$E(2)_{\text{synclinal/anti}}$	18.48	23.96	21.32	25.11
$E(2)_{\text{synclinal/anti}}$ $a \rightarrow g$		5.48		3.79
$E(\text{del})_{\text{synclinal/anti}}$	17.38	21.98	20.17	22.96
$E(\text{del})_{\text{synclinal/anti}}$ $a \rightarrow g$		4.60		2.78
***Anti* hyperconjugation**				
C–H → C–H*	2.59 (×4)	2.81 (×2)	3.08 (×2)	3.15
			2.73 (×2)	2.95
C–F → C–Y*	1.80		2.22	
C–Y → C–F*	1.80		3.76	
C–H → C–F*		5.81		5.46
C–H → C–Y*		5.81		6.82
C–F → C–H*		0.85		1.06
C–Y → C–H*		0.85		1.91
Total $E(2)_{\text{anti}}$	13.96	18.94	17.60	21.35
Total $E(2)_{\text{anti}}$ $a \rightarrow g$		4.98		3.75

to the *anti* → *gauche* conformational isomerization in CFE with respect to that in DFE.

Thus, it is a drop in electrostatic and orbital stabilizing interactions which is responsible for the *anti* preference of isolated CFE. Despite the expected electrostatic repulsion between the two C–F bond dipoles in DFE and the C–F and C–Cl bond dipoles in CFE in their *gauche* conformers, they are actually more stabilized by electrostatic interactions than the *anti* forms. Somewhat counterintuitively, this stabilization is larger in DFE ($\Delta E_{\text{elstat}} = -3.38$ kcal mol^{-1}, Table 1) than in CFE ($\Delta E_{\text{elstat}} = -0.82$ kcal mol^{-1}, Table 1). These findings lead to conclusion that small electronegative atom, such as fluorine, contributes more electrostatic stabilization to the *anti* → *gauche* isomerization than does the less electronegative and bulkier atom, such as chlorine. The above conclusion also supports an earlier explanation of the *gauche* effect in terms of electrostatic interactions.[4] Though, orbital interactions are important, too.

2-Fluoroethanol, 2-chloroethanol and their protonated forms

The MP2/6-311++G** geometry optimizations of 2-fluoroethanol (FE) and 2-chloroethanol (CE) led to the five energetically distinguishable minima, shown in Fig. 2 along with their relative electronic energies. They are denoted as *aa*, *ag*, *ga*, *gg* and *gg*′, where the first letter refers to the heavy atom F(Cl)–C–C–O conformation, the second to the C–C–O–H conformation. The *ag* and *ag*′ conformers are mirror images and energetically indistinguishable. They are both included in discussion to be compared with the corresponding *gg* and *gg*′ forms. Optimized geometrical parameters for all conformers of FE and CE are given in Tables S3 and S4 in the ESI.† They compare well with the available experimental data from electron diffraction studies.[12a,19a] The most stable forms for both FE and CE are *gg*′ having a hydroxyl hydrogen atom pointing toward the halogen atom in the heavy atom *gauche* arrangement. The *anti* conformers of FE are by 2.3 and 2.5 kcal mol^{-1} higher in energy and this is consistent with previous experimental and theoretical studies.[12] The energy difference between *gg*′ form of CE and *anti* conformers is smaller and amounts ~1.7 kcal mol^{-1}, at the employed theory level. This is also in accord with previous experimental and theoretical data.[12d,f,g,19]

In the following, the energy change accompanying *anti* → *gauche* rotation is analyzed as the energy difference between *gauche* conformers and their corresponding *anti* conformers, having the same conformational arrangement around the C–O bonds (*anti*, + *gauche* or − *gauche*, Fig. 2). Decomposition of the total binding energy between two radical fragments into its components is given in Table 3, along with the decomposition of energy change upon *anti* → *gauche* rotation. Stabilization energies due to the vicinal total (*synclinal* and *anti*) and *anti* hyperconjugative interactions between the two XCH_2 and CH_2OH units, evaluated by the NBO analysis, are listed in Table 4, including also energy changes following the *anti* → *gauche* conformational isomerization.

The rotation of *aa*-FE into the corresponding *gauche* form, that is *aa*-FE → *ga*-FE (Fig. 2 and Table 3), results in a very small *gauche* preference of $\Delta E = -0.15$ kcal mol^{-1}, whereas the *ag*-FE → *gg*-FE rotation slightly increases the energy of the system by $\Delta E = 0.09$ kcal mol^{-1}. The true *gauche* stabilization occurs only upon *ag*′-FE → *gg*′-FE rotation, $\Delta E = -2.54$ kcal mol^{-1}. These findings compare with the results of Briggs *et al.*,[12e] which led authors to conclude that *gauche* effect in FE does not have its origin in stereoelectronic effects, but comes from intramolecular hydrogen bonding stabilization. An inspection of data in Tables 3 and 4, however, show that *anti* hyperconjugative interactions (total $E(2)_{\text{anti}}$ $a \rightarrow g$ in Table 4), all vicinal hyperconjugative interactions ($E(2)_{\text{synclinal/anti}}$ $a \rightarrow g$ and $E(\text{del})_{\text{synclinal/anti}}$ $a \rightarrow g$ in Table 4) and all orbital interactions (ΔE_{pol} in Table 3) become stronger during the all three rotations. Thus, there exists stereoelectronic *gauche* effect in FE. The most important *anti* hyperconjugative interactions in *gauche* structures are C–H → C–F* and C–H → C–O*, the former being more pronounced (Table 4). This arises from a combination of two factors: lower energy of the C–F* orbital and its larger polarization toward the neighbouring carbon atom, due to the larger electronegativity of fluorine atom. The latter allows a stronger orbital overlap.[6b] The electrostatic energy term ΔE_{elstat} becomes more stabilizing for all three conformational changes, which is also the case for dispersion interactions ΔE_{disp}, though with smaller magnitude (Table 3). For the *aa*-FE → *ga*-FE rotation, these stabilizing interactions are not large enough to override a destabilization coming from the increase in the steric repulsion (which is the strongest in this case), thus making the ΔE_{int} positive (0.33 kcal mol^{-1}). The slight *gauche* preference for this rotation actually comes from an energy loss due to the accompanying structural changes, $\Delta E_{\text{prep}} = -0.48$ kcal mol^{-1}. In the case of *ag*-FE → *gg*-FE conformational change, the interaction energy becomes more stabilizing, $\Delta E_{\text{int}} = -0.66$ kcal mol^{-1}, but not enough to overcome the increase in the $\Delta E_{\text{prep}} = 0.75$ kcal mol^{-1} and there is almost no conformational preference for this

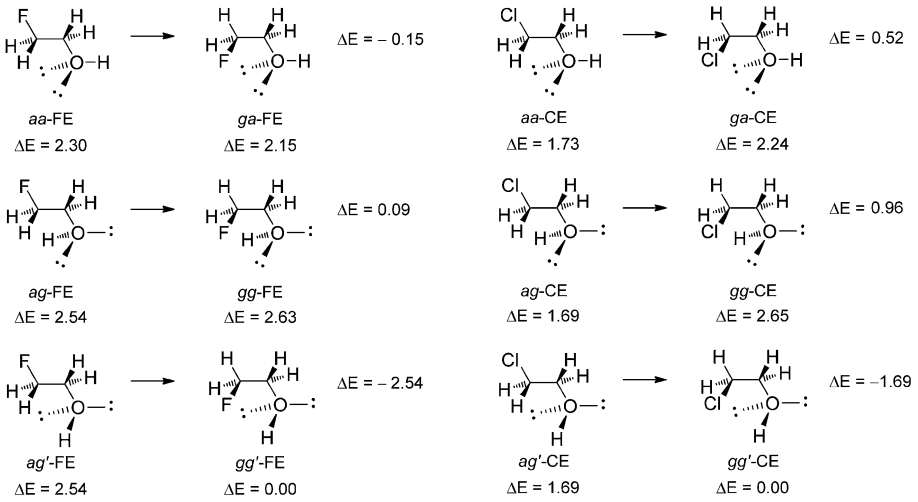

Fig. 2 Energy minimum conformations of 2-fluoroethanol (FE) and 2-chloroethanol (CE), their relative electronic energies (kcal mol^{-1}) and energy changes occurring upon *anti* → *gauche* rotation of the heavy atom chain.

rotation. The pronounced *gauche* stabilization for *ag*′-FE → *gg*′-FE rotation of $\Delta E = -2.54$ kcal mol^{-1} results from a favourable interaction energy, $\Delta E_{int} = -3.11$ kcal mol^{-1}, while ΔE_{prep} rises by 0.57 kcal mol^{-1}. The interaction energy stabilization owes mainly to the electrostatic energy $\Delta E_{elstat} = -5.34$ kcal mol^{-1}, followed by the orbital interaction energy $\Delta E_{pol} = -3.03$ kcal mol^{-1}. The dispersion energy contribution is significantly smaller, $\Delta E_{disp} = -0.51$ kcal mol^{-1} (Table 3). Hence, even in the neutral FE, the most important contributor to the *gauche* effect is electrostatic energy. A part of electrostatic stabilization should be ascribed to the attraction between the two antiparallel C–F and O–H bond dipoles, with $\theta_{FCOH} = 4.3°$. However, other electrostatic stabilizing interactions must be involved, too, since ΔE_{elstat} becomes more stabilizing even for the remaining two rotations which bring fluorine atom near the oxygen lone pair. In these cases, an electrostatic repulsion between the C–F and C–O bond dipoles and between fluorine and oxygen lone pairs is anticipated. Our results, however, once again point out that partial interaction between bond pairs and lone pairs is not always enough to account for the overall change in electrostatic interactions.

Now, let us examine what happens when fluorine atom is replaced with the less electronegative and larger chlorine atom. Both *aa*-CE → *ga*-CE and *ag*-CE → *gg*-CE rotations are followed by an increase in energy by $\Delta E = 0.52$ and $\Delta E = 0.96$ kcal mol^{-1}, respectively, which is due to the $\Delta E_{int} = 1.14$ kcal mol^{-1} in the first case, $\Delta E_{int} = 0.20$ kcal mol^{-1} and $\Delta E_{prep} = 0.76$ kcal mol^{-1} in the second case. The favourable preparation energy for the former isomerization reduces the interaction energy rise by $\Delta E_{prep} = -0.62$ kcal mol^{-1} (Table 3). The *ag*′-CE → *gg*′-CE rotation still leads to *gauche* preference, though smaller than in FE ($\Delta E = -1.69$ kcal mol^{-1} for CE and $\Delta E = -2.54$ kcal mol^{-1} for FE,

Table 3 Contribution of various energy terms to the total binding interactions between two $XH_2C^{\bullet}$ and $^{\bullet}CH_2OH$ radicals and to the *anti* → *gauche* energy change in 2-fluoroethanol (FE, X = F) and 2-chloroethanol (CE, X = Cl).[a] Values are in kcal mol^{-1}

Conformation	ΔE_{elstat}	ΔE_{ex+rep}	ΔE_{pol}	ΔE_{disp}	ΔE_{int}	ΔE_{prep}	ΔE
aa-FE	−150.80	221.88	−154.60	−27.69	−111.21	17.22	−93.99
ag-FE	−155.52	233.81	−157.32	−25.64	−104.67	10.91	−93.76
ga-FE	−153.53	229.18	−158.42	−28.11	−110.88	16.74	−94.14
gg-FE	−156.80	237.67	−159.87	−26.33	−105.33	11.66	−93.67
gg′-FE[b]	−160.86	239.58	−160.35	−26.15	−107.78	11.48	−96.30
aa-FE → *ga*-FE	−2.73	7.30	−3.82	−0.42	0.33	−0.48	−0.15
ag-FE → *gg*-FE	−1.28	3.86	−2.55	−0.69	−0.66	0.75	0.09
ag′-FE → *gg*′-FE	−5.34	5.77	−3.03	−0.51	−3.11	0.57	−2.54
aa-CE	−150.42	224.13	−155.33	−31.35	−112.97	19.14	−93.83
ag-CE	−155.07	235.40	−157.47	−29.33	−106.47	12.61	−93.86
ga-CE	−151.71	229.20	−157.58	−31.74	−111.83	18.52	−93.31
gg-CE	−154.48	236.57	−158.39	−29.97	−106.27	13.37	−92.90
gg′-CE[b]	−158.52	239.37	−159.48	−29.99	−108.62	13.08	−95.54
aa-CE → *ga*-CE	−1.29	5.07	−2.25	−0.39	1.14	−0.62	0.52
ag-CE → *gg*-CE	0.59	1.17	−0.92	−0.64	0.20	0.76	0.96
ag′-CE → *gg*′-CE	−3.45	3.97	−2.01	−0.66	−2.15	0.46	−1.69

[a] Labeling of various energy terms is the same as in Table 1. [b] Structure having the OH hydrogen atom oriented toward a halogen atom.

Table 4 Energies (in kcal mol^{-1}) of vicinal hyperconjugative interactions in 2-fluoroethanol (FE, X = F) and 2-chloroethanol (CE, X = Cl) estimated from the second-order perturbative approach, $E(2)$ values, and deletion of the corresponding Fock matrix elements in the NBO basis, E(del). Calculated at the HF/6-311++G** level

	FE					CE				
	aa	*ag*	*ga*	*gg*	*gg′*	*aa*	*ag*	*ga*	*gg*	*gg′*
Vicinal hyperconjugation										
$E(2)_{\text{synclinal/anti}}$	19.33	19.20	23.06	23.79	23.14	21.84	21.59	24.67	25.28	24.98
$E(2)_{\text{synclinal/anti}}$ $a \rightarrow g$			3.73	4.59	3.94			2.83	3.69	3.39
$E(\text{del})_{\text{synclinal/anti}}$	18.13	18.05	21.23	21.94	21.34	20.56	20.46	22.56	23.16	22.84
$E(\text{del})_{\text{synclinal/anti}}$ $a \rightarrow g$			3.10	3.88	3.28			2.00	2.70	2.38
***Anti* hyperconjugation**										
C–H → C–H*	2.81	2.85	2.92	2.97	3.01	2.95	2.96	3.14	3.02	3.03
	2.78	2.74	2.85	3.27	3.10	2.95	2.82	3.17	3.65	3.42
	2.74	2.73				3.18	3.15			
	2.73	2.97				3.18	3.47			
C–X → C–O*	1.57	1.70				3.15	3.44			
C–O → C–X*	2.29	2.06				2.91	2.56			
C–H → C–X*			5.79	6.15	5.95			7.01	7.29	7.26
C–H → C–O*			4.63	5.51	4.89			4.36	5.28	4.85
C–X → C–H*			0.94	0.92	1.07			2.01	1.93	2.13
C–O → C–H*			1.02	0.85	0.98			1.28	1.00	1.12
Total $E(2)_{\text{anti}}$	14.92	15.05	18.15	19.67	19.00	18.32	18.40	20.97	22.17	21.81
Total $E(2)_{\text{anti}}$ $a \rightarrow g$			3.23	4.62	3.95			2.65	3.77	3.41

Fig. 2 and Table 3). This is due to the $\Delta E_{\text{int}} = -2.15$ kcal mol^{-1}, while ΔE_{prep} increases the energy by 0.46 kcal mol^{-1} (and is smaller compared to the corresponding rotation of FE, with $\Delta E_{\text{prep}} = 0.57$ kcal mol^{-1}).

An examination of data in Table 3 enables us to explain the observed changes in ΔE_{int} during the three rotations of CE and its smaller *gauche* effect (*ag′*-CE → *gg′*-CE isomerization) compared to that in FE. Similarly as in the case of CFE, the interaction energy rise (positive ΔE_{int} for the first two rotations) and its smaller negative change for the third rotation do not have their origin in the steric effect. The increase in the $\Delta E_{\text{ex+rep}}$ is smaller for CE than for FE for all three rotations. Again, electrostatic and orbital stabilizing interactions are smaller for the *anti* → *gauche* rotation in CE compared to FE (change in ΔE_{elstat} is even destabilizing (positive) for the *ag*-CE → *gg*-CE rotation). This decrease in the ΔE_{elstat} and ΔE_{pol} makes the ΔE_{int} energy term positive for the *aa*-CE → *ga*-CE and *ag*-CE → *gg*-CE conformational changes, and less negative (by ∼1 kcal mol^{-1}) for the *ag′*-CE → *gg′*-CE isomerization relative to the *ag′*-FE → *gg′*-FE one. For all three rotations, dispersion energies are favourable, though their stabilizing effect does not exceed 0.7 kcal mol^{-1}. Thus, as in the case of CFE, the less electronegative and larger chlorine atom provides smaller electrostatic and orbital stabilization to the *anti* → *gauche* conformational change, compared to fluoroalcohol.

A part of a decrease in the orbital interaction energy can be analyzed by examination of the NBO results shown in Table 4. Total and *anti* vicinal hyperconjugative stabilization associated with the *anti* → *gauche* isomerization is smaller in CE than in FE. This should be ascribed to larger increase in hyperconjugation in *anti* forms of CE than in *gauche* forms relative to FE. The increase in the hyperconjugative stabilization in *anti* conformers of CE mainly stems from the more favourable C–Cl → C–O* interaction (3.2–3.4 kcal mol^{-1}) *vs.* C–F → C–O* interaction (1.6–1.7 kcal mol^{-1}) in FE, consistent with the better electron-donating ability of the C–Cl bond, as already mentioned above. There are also contributions from other interactions, but smaller in magnitude. In the case of *gauche* conformers, main contribution to larger hyperconjugative stabilization comes from an increase in the C–H → C–Cl* (7–7.3 kcal mol^{-1}) and C–Cl → C–H* interactions (1.9–2.1 kcal mol^{-1}) in CE *vs.* C–H → C–F* (5.8–6.2 kcal mol^{-1}) and C–F → C–H* (0.9–1.1 kcal mol^{-1}) in FE, and this compares with the results for CFE *vs.* DFE (Tables 2 and 4). Thus, the *anti* → *gauche* isomerization benefits less from hyperconjugation in the case of CE compared to FE.

Overall, the *gauche* effect in CE, observed for the *ag′*-CE → *gg′*-CE isomerization, has to be ascribed to electrostatic energy as the main stabilizing factor ($\Delta E_{\text{elstat}} = -3.45$ kcal mol^{-1}), orbital interaction energy ($\Delta E_{\text{pol}} = -2.01$ kcal mol^{-1}) and dispersion energy ($\Delta E_{\text{disp}} = -0.66$ kcal mol^{-1}). In this case, too, a part of electrostatic stabilization should be attributed to the attraction between the nearly parallel, but oppositely oriented C–Cl and O–H bond dipoles, with $\theta_{\text{ClCOH}} = 3°$.

The protonated FE and CE, abbreviated herein as FEH and CEH, respectively, can exist as five energetically distinguishable conformers denoted as *aa*, *ag*, *ga*, *gg* and *gg′*, where the first letter refers to the heavy atom F(Cl)–C–C–O conformation, the second to the C–C–O–: conformation They are shown in Fig. 3, along with their relative energies. The *ag′* conformer is enantiomeric with the *ag* one, and is included in the discussion for comparison with the corresponding *gg′* conformer. As with the neutral alcohols, energies of *gauche* conformers are analyzed with respect to their corresponding *anti* forms (Fig. 3). The

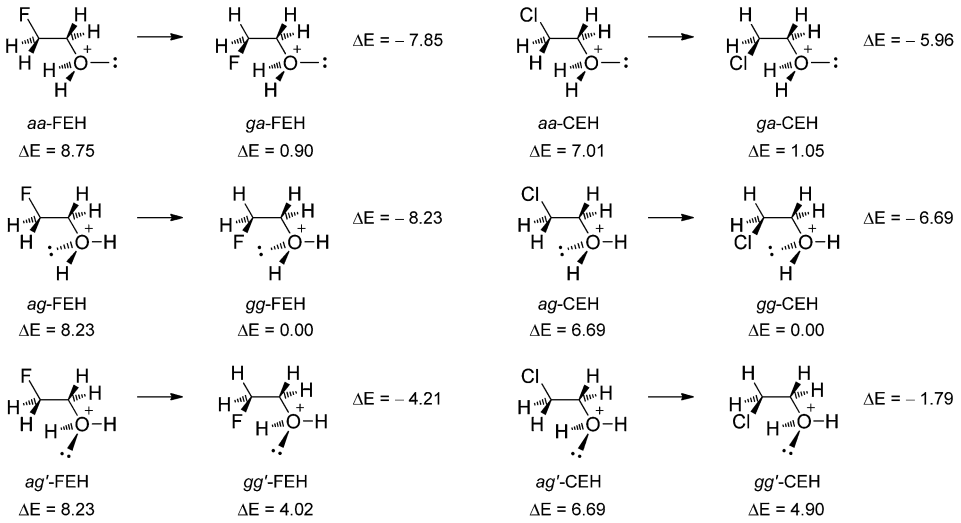

Fig. 3 Energy minimum conformations of protonated 2-fluoroethanol (FEH) and protonated 2-chloroethanol (CEH), their relative electronic energies (kcal mol^{-1}) and energy changes occurring upon *anti* → *gauche* rotation of the heavy atom chain.

optimized structural parameters for FEH and CEH are given in Tables S5 and S6 in the ESI.†

The protonated FE shows very large *gauche* preference for all three rotations (*aa*-FEH → *ga*-FEH, *ag*-FEH → *gg*-FEH, *ag*′-FEH → *gg*′-FEH), particularly pronounced when *gauche* forms have a hydroxyl hydrogen atom oriented toward the fluorine atom (the first two rotations in Fig. 3). These findings are consistent with previous study on protonated FE,[12e] which led authors to conclude that in this case the *gauche* effect originates from both intramolecular hydrogen bonding stabilization and stereoelectronic effects. The latter was seen as the only stabilization in the *ag*′-FEH → *gg*′-FEH rotation, since there is no hydrogen bond in the *gg*′ conformation.[12e] Our energy decomposition and NBO data reveal that all orbital stabilization (ΔE_{pol} in Table 5), as well as *anti* and total vicinal hyperconjugation (Table 6) are indeed larger in *gauche* conformations by 5.3–5.8 kcal mol^{-1}, 3.3–6.4 kcal mol^{-1} and 3.7–6.7 kcal mol^{-1}, respectively. Among the *anti* hyperconjugative interactions, the most important one contributing to the stabilization of the *gauche* forms is the C–H → C–O* interaction, having stabilizing energy of 6.4–9 kcal mol^{-1}. The C–H → C–F* interaction contributes smaller stabilizing energy of 3.5–4.1 kcal mol^{-1}. Thus, protonation of hydroxy group enhances electron-accepting ability of the C–O* antibond and reverses the relative strength of C–H → C–F* and C–H → C–O* interactions in neutral and protonated alcohols. This enhancement arises from the C–O* antibond energy lowering and larger polarization. Our conclusions, thus, agree with those of Briggs *et al.*[12e] that there exists stereoelectronic *gauche* effect in protonated FE.

Table 5 Contribution of various energy terms to the total binding interactions between two $XH_2C^{\bullet}$ and $^{\bullet}CH_2OH_2^{+}$ units and to the *anti* → *gauche* energy change in protonated 2-fluoroethanol (FEH, X = F) and protonated 2-chloroethanol (CEH, X = Cl).[a] Values are in kcal mol^{-1}

Conformation	ΔE_{elstat}	ΔE_{ex+rep}	ΔE_{pol}	ΔE_{disp}	ΔE_{int}	ΔE_{prep}	ΔE
aa-FEH	−128.96	202.24	−154.75	−28.01	−109.48	9.46	−100.02
ag-FEH	−128.21	198.90	−154.83	−28.43	−112.57	12.03	−100.54
ga-FEH[b]	−141.80	211.84	−160.01	−28.17	−118.14	10.27	−107.87
gg-FEH[b]	−140.53	208.42	−160.23	−29.27	−121.61	12.84	−108.77
gg′-FEH	−135.09	207.31	−160.65	−29.15	−117.58	12.83	−104.75
aa-FEH → *ga*-FEH	−12.84	9.60	−5.26	−0.16	−8.66	0.80	−7.86
ag-FEH → *gg*-FEH	−12.32	9.52	−5.40	−0.84	−9.04	0.81	−8.23
ag′-FEH → *gg*′-FEH	−6.88	8.41	−5.82	−0.72	−5.01	0.80	−4.21
aa-CEH	−132.52	212.11	−162.00	−32.47	−114.88	11.86	−103.02
ag-CEH	−131.86	209.34	−162.31	−33.04	−117.87	14.53	−103.34
ga-CEH[b]	−142.38	221.24	−166.33	−34.33	−121.80	12.82	−108.98
gg-CEH[b]	−141.34	218.99	−167.35	−35.65	−125.35	15.32	−110.03
gg′-CEH	−134.52	211.04	−163.05	−33.85	−120.38	15.26	−105.12
aa-CEH → *ga*-CEH	−9.86	9.13	−4.33	−1.86	−6.92	0.96	−5.96
ag-CEH → *gg*-CEH	−9.48	9.65	−5.04	−2.61	−7.48	0.79	−6.69
ag′-CEH → *gg*′-CEH	−2.66	1.70	−0.74	−0.81	−2.51	0.72	−1.79

[a] Labeling of various energy terms is the same as in Table 1. [b] Structure having an OH_2^{+} hydrogen atom oriented toward a halogen atom.

Table 6 Energies (in kcal mol^{-1}) of vicinal hyperconjugative interactions in protonated 2-fluoroethanol (FEH, X = F) and protonated 2-chloroethanol (CEH, X = Cl) estimated from the second-order perturbative approach, $E(2)$ values, and deletion of the corresponding Fock matrix elements in the NBO basis, E(del). Calculated at the HF/6-311++G** level

	FEH					CEH				
	aa	*ag*	*ga*	*gg*	*gg′*	*aa*	*ag*	*ga*	*gg*	*gg′*
Vicinal hyperconjugation										
$E(2)_{\text{synclinal/anti}}$	18.64	18.48	22.77	22.17	25.23	24.99	24.77	25.06	24.56	27.67
$E(2)_{\text{synclinal/anti}}$ $a \rightarrow g$			4.13	3.69	6.75			0.07	−0.21	2.90
$E(\text{del})_{\text{synclinal/anti}}$	17.63	17.40	20.76	20.19	22.73	23.26	22.95	22.87	22.36	24.93
$E(\text{del})_{\text{synclinal/anti}}$ $a \rightarrow g$			3.13	2.80	5.33			−0.39	−0.59	1.97
***Anti* hyperconjugation**										
C–H → C–H*	2.74	2.67	2.83	2.88	2.94	3.10	3.03	2.80	2.92	3.18
	2.74	2.76	2.45	2.21	2.47	3.10	3.16	2.89	2.64	2.89
	2.10	2.07				2.70	2.73			
	2.10	1.87				2.70	2.43			
C–X → C–O*	3.44	3.20				8.46	7.99			
C–O → C–X*	1.22	1.34				1.55	1.72			
C–H → C–X*			3.53	3.66	4.08			4.55	4.75	5.12
C–H → C–O*			7.22	6.37	8.97			7.45	6.66	9.33
C–X → C–H*			1.22	1.17	1.04			2.47	2.36	2.22
C–O → C–H*			0.87	0.95	0.83			1.00	1.13	1.03
Total $E(2)_{\text{anti}}$	14.34	13.91	18.12	17.24	20.33	21.61	21.06	21.16	20.46	23.77
Total $E(2)_{\text{anti}}$ $a \rightarrow g$			3.78	3.33	6.42			−0.45	−0.60	2.71

Energy decomposition data, given in Table 5, reveal which other factors contribute to the very strong *gauche* preference in FEH. Thus, in all three isomerizations it results from ΔE_{int}, while ΔE_{prep} increases by 0.8 kcal mol^{-1}. Major factor which is responsible for the large *gauche* conformer stabilization in the *aa*-FEH → *ga*-FEH and *ag*-FEH → *gg*-FEH rotations is a very favourable electrostatic energy component, which reaches values of 12.84 kcal mol^{-1} and 12.32 kcal mol^{-1}, respectively (ΔE_{elstat} in Table 5). Electrostatic stabilization energy is smaller, but still significant for the *ag′*-FEH → *gg′*-FEH conformational change, 6.88 kcal mol^{-1}. In the first two cases, the large electrostatic stabilization partly arises from an attraction between the two almost antiparallel O–H and C–F bond dipoles, having θ_{FCOH} 6.4° and 8.1°, respectively. There are, however, other attractive contributions, since the electrostatic energy becomes more favourable even for the third rotation, when the *gauche* form is expected to be destabilized by the repulsion between the two C–O and C–F bond dipoles. The calculated NBO charges showed that the positive charge in the C–OH_2^+ fragment is distributed on hydrogen and carbon atoms whereas the oxygen contains the negative charge. In addition, electrostatic repulsion between lone pairs should be involved, too.

To conclude, the ΔE_{elstat} energy component provides the most important contribution to the *gauche* effect in FEH. Next comes the orbital interaction energy, which ranges from 5.2–5.8 kcal mol^{-1}. They both, along with the much smaller ΔE_{disp}, 0.2–0.8 kcal mol^{-1} make the ΔE_{int} very favourable, by strongly overcoming the also prominent increase in the steric repulsion (8.4–9.6 kcal mol^{-1}).

Our extension to chloro derivatives shows that protonation of CE also leads to the pronounced *gauche* preference of 6–6.7 kcal mol^{-1} (Fig. 3 and Table 5) compared to only 1.7 kcal mol^{-1} in the neutral alcohol (Fig. 2 and Table 3), taking into account conformational changes leading to the *gauche* structures having a hydroxyl hydrogen atom oriented toward the chlorine atom (*aa*-CEH → *ga*-CEH and *ag*-CEH → *gg*-CEH rotations for the protonated alcohol, and *ag′*-CE → *gg′*-CE rotation for the alcohol). Contrary to the neutral CE, the protonated molecule also shows *gauche* stabilization for the *ag′*-CEH → *gg′*-CEH rotation when chlorine atom becomes oriented toward the oxygen lone pair. The energy of this stabilization is smaller and amounts $\Delta E = -1.79$ kcal mol^{-1}. For all three rotations, depicted in Fig. 3, it is the ΔE_{int} that favours the conformational change (2.5–7.5 kcal mol^{-1}), whereas structural changes lead to an increase in energy by 0.7–1 kcal mol^{-1} (Table 5). The most important factor that makes ΔE_{int} more negative is ΔE_{elstat}, for all three rotations. There is a strong electrostatic stabilization for the *aa*-CEH → *ga*-CEH and *ag*-CEH → *gg*-CEH conformational changes which amounts 9.86 kcal mol^{-1} and 9.48 kcal mol^{-1}, respectively, and the smaller one for the *ag′*-CEH → *gg′*-CEH rotation of 2.66 kcal mol^{-1}, but still stabilizing despite the expected lone pairs repulsion and C–Cl/C–O bond dipoles repulsion. As with the fluoro derivative, the oxygen atom is the negative part of the C–O bond dipole in the C–OH_2^+ unit. The next stabilizing effect comes from orbital interactions and dispersion energy term which is by ~1.7 kcal mol^{-1} stronger than in FEH, for the first two isomerizations. The ΔE_{pol} for the *aa*-CEH → *ga*-CEH (4.33 kcal mol^{-1}) and *ag*-CEH → *gg*-CEH (5.04 kcal mol^{-1}) rotations is significantly greater than that for the *ag′*-CEH → *gg′*-CEH rotation (0.74 kcal mol^{-1}), while the NBO results show that there is no hyperconjugative stabilization following the first two rotations (Table 6), which should be

ascribed mainly to strong C–Cl → C–O* interaction in *anti* conformers (8–8.5 kcal mol^{-1}, compared to 3.2–3.4 kcal mol^{-1} for the C–F → C–O* interaction in FEH). The third isomerization is the only one that has stereoelectronic origin, in addition to other orbital effects. Thus, the more favourable ΔE_{pol} component observed for the *aa*-CEH → *ga*-CEH and *ag*-CEH → *gg*-CEH rotations, which compares with the corresponding values for FEH, should be related to polarization effects and charge transfer in hydrogen bonding interactions. Indeed, the NBO(del) calculations revealed a very large charge transfer component of hydrogen bonding in *ga*-CEH and *gg*-CEH, which amount 10.6 kcal mol^{-1} and 13.3 kcal mol^{-1}, respectively. This has to be compared with only 1.2 kcal mol^{-1} and 2 kcal mol^{-1} for *ga*-FEH and *gg*-FEH, 0.6 kcal mol^{-1} for *gg*′-CE and 0.2 kcal mol^{-1} for *gg*′-FE. Though, it should be noted that NBO overestimates charge transfer interactions compared to the BLW method,[28,40] but their trend is the same.[39]

The steric strain arising from the closer contact between Cl and OH_2^+ substituents in *gauche* conformers is very similar to that observed for FEH regarding the *aa*-CEH → *ga*-CEH and *ag*-CEH → *gg*-CEH rotations, and significantly smaller for the *ag*′-CEH → *gg*′-CEH change (Table 5). This means that the decreased *gauche* effect in CEH compared to that in FEH does not originate from steric effects, but from a decrease in electrostatic stabilizing energy, which is 12.3–12.8 kcal mol^{-1} for the first two rotations in FEH, but 9.5–9.9 kcal mol^{-1} for the same conformational changes in CEH. There is a drop in this energy term for the third *ag*′-CEH → *gg*′-CEH rotation, as well (6.9 kcal mol^{-1} for FEH and 2.7 kcal mol^{-1} for CEH). A drop in the orbital interactions is less pronounced except for the *ag*′-CEH → *gg*′-CEH rotation, lacking the intramolecular hydrogen bond (Table 5). Therefore, only for the *ag*′ → *gg*′ conformational change the stronger *gauche* preference in FEH owes to both electrostatic and orbital stabilizing interactions. In the case of the other two *aa* → *ga* and *ag* → *gg* isomerizations, the larger *gauche* effect in FEH originates mostly from more favourable electrostatic energy.

2-Fluoroethylamine, 2-chloroethylamine and their protonated forms

The MP2/6-311++G** geometry optimizations of 2-fluoroethylamine (FEA) and 2-chloroethylamine (CEA) led to the five energetically distinguishable minima, depicted in Fig. 4 along with their relative electronic energies. They are denoted as *aa*, *ag*, *ga*, *gg* and *gg*′, where the first letter refers to the heavy atom F(Cl)–C–C–N conformation and the second to the C–C–N–: conformation. Here, again, the enantiomeric *ag* and *ag*′ conformers are both included to be compared with the corresponding *gg* and *gg*′ forms. Optimized geometrical parameters for all conformers of FEA and CEA are given in Tables S7 and S8 in the ESI.† For FEA, they are in good agreement with the available experimental data.[13d] The two most stable conformers for both FEA and CEA are those having one of amino hydrogen atoms pointing toward the halogen atom in the heavy atom *gauche* arrangement. Among them, the *gg* form is slightly more stable than the *ga* form. In the case of FEA, this agrees with previous experimental[13a,d] and theoretical studies.[13c] The relative energies of five conformers of FEA are also in accord with the existing experimental data,[13d] though the energy difference between the *aa* and *ag* forms is small (0.12 kcal mol^{-1}) and their relative stability may vary with the level of computations.[13c] The same applies to CEA, for which *aa* and *ag* conformers differ by 0.17 kcal mol^{-1} in our calculations. Conformers *ga*-CEA and *gg*-CEA also have similar energies which is in accord with previous experimental and theoretical data,[20] although their relative stability order is reversed in our MP2 calculations. The relative energies for other three conformers of CEA are in agreement with the exisiting data.[20] As in the case of 2-haloalcohols, the *gauche* preference in amines is smaller when halogen is chlorine atom.

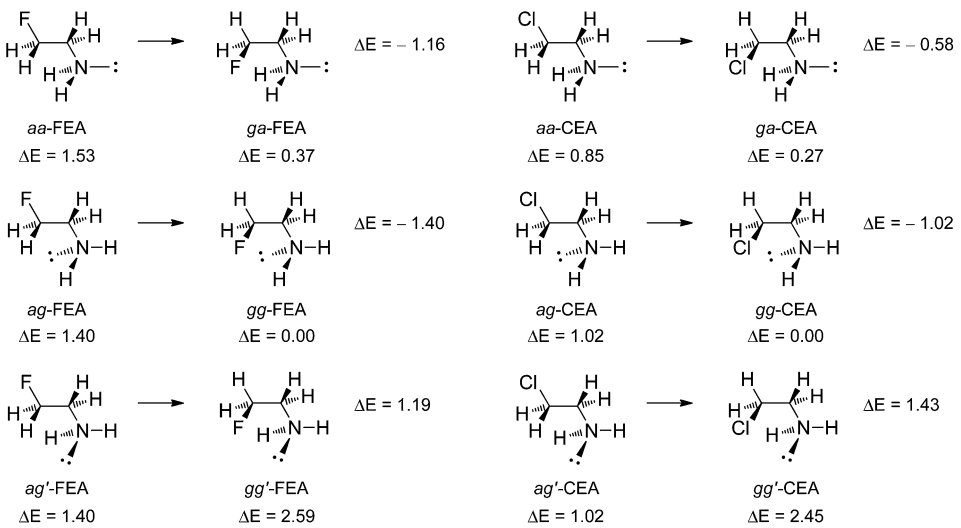

Fig. 4 Energy minimum conformations of 2-fluoroethylamine (FEA) and 2-chloroethylamine (CEA), their relative electronic energies (kcal mol^{-1}) and energy changes occurring upon *anti* → *gauche* rotation of the heavy atom chain.

Decomposition of the total binding energy between the two $XCH_2^{\bullet}$ and $^{\bullet}CH_2NH_2$ radical fragments into its components is given in Table 7, along with the decomposition of energy change occurring upon *anti* → *gauche* rotation of the heavy atom chain. Stabilization energies due to the vicinal *anti* hyperconjugative interactions and all vicinal hyperconjugative interactions (*synclinal* and *anti*) between the two XCH_2 and CH_2NH_2 units, evaluated by the NBO analysis, are listed in Table 8, including energy changes following *anti* → *gauche* conformational isomerization (denoted as *a* → *g*).

In the case of FEA, the *aa*-FEA → *ga*-FEA and *ag*-FEA → *gg*-FEA conformational isomerizations lead to a decrease in energy (stabilization of the system) by $\Delta E = -1.16$ kcal mol^{-1} and $\Delta E = -1.40$ kcal mol^{-1}, respectively. This has to be ascribed to the ΔE_{int}, while ΔE_{prep} increases by 0.34 kcal mol^{-1} and 1.93 kcal mol^{-1}, respectively. For the first rotation, $\Delta E_{elstat} = -2.71$ kcal mol^{-1} is more stabilizing than $\Delta E_{pol} = -1.17$ kcal mol^{-1}, while dispersion energy contribution is negligible (Table 7). For the second rotation, $\Delta E_{pol} = -1.62$ kcal mol^{-1} is slightly more favourable than $\Delta E_{elstat} = -1.46$ kcal mol^{-1}, and the dispersion energy stabilizing contribution increases to $\Delta E_{disp} = -0.69$ kcal mol^{-1}. In both cases, these stabilizing interactions overcome the increase in the steric repulsion, introduced mostly by bringing the two substituents into the *gauche* position. Thus, the *gauche* preference in FEA should be ascribed to both electrostatic and orbital stabilizing interactions. Data in Table 8 show that vicinal hyperconjugative interactions between the two FCH_2 and CH_2NH_2 fragments also become stabilizing upon *aa*-FEA → *ga*-FEA and *ag*-FEA → *gg*-FEA isomerizations, meaning that stereoelectronic effects contribute to the *gauche* stabilization, too. The most important hyperconjugative interactions that stabilize the *gauche* forms are C–H → C–F* (~6 kcal mol^{-1}) and C–H → C–N* (4.1–4.9 kcal mol^{-1}).

The third *ag*′-FEA → *gg*′-FEA rotation does not result in molecule stabilization, that is it increases the energy by $\Delta E = 1.19$ kcal mol^{-1}, both because of an increase in ΔE_{int} and ΔE_{prep} (Fig. 4 and Table 7). The stabilizing stereoelectronic effects, as well as all orbital stabilizing interactions are still present, as evidenced from the data in Tables 7 (ΔE_{pol}) and 8. The increase in the steric repulsion does not exceed values for the first two isomerizations. What is missing now is more stabilizing electrostatic interaction, since ΔE_{elstat} becomes less favourable (positive) by 1.22 kcal mol^{-1}. This differs from the case of FE, when electrostatic energy favours *gauche* conformation even when fluorine atom encounters oxygen lone pairs (compare data for *aa*-FE → *ga*-FE and *ag*-FE → *gg*-FE rotations in Table 3 with those for *ag*′-FEA → *gg*′-FEA rotation in Table 7). This reinforces our above mentioned conclusion that the favourable electrostatic energy change is more important for smaller and more electronegative atoms. Though, in this case van der Waals radii do not differ much (1.55 Å for N, 1.52 Å for O),[21] but electronegativity between N and O atoms differs by 0.5 according to the Pauling electronegativity scale.

The conformational behaviour of CEA resembles the behavior of FEA in that the *aa*-CEA → *ga*-CEA and *ag*-CEA → *gg*-CEA isomerizations are followed by a decrease in energy by $\Delta E = -0.58$ kcal mol^{-1} and $\Delta E = -1.02$ kcal mol^{-1}, respectively, whereas the *ag*′-CEA → *gg*′-CEA rotation results in an increase in energy by $\Delta E = 1.43$ kcal mol^{-1} (Fig. 4 and Table 7). In all three cases ΔE_{prep} becomes more positive, so that *gauche* stabilization in the first two isomerizations results from the more favourable ΔE_{int}. In the latter case, ΔE_{int} increases, as well. The energetic stabilization of the system (*gauche* preference) is smaller than in FEA, while energetic destabilization following the *ag*′-CEA → *gg*′-CEA rotation is larger than in FEA. The reason for this lies in the ΔE_{int} energy, since increase in ΔE_{prep} is smaller than in FEA. The *aa*-CEA → *ga*-CEA isomerization owes more to the electrostatic stabilization, $\Delta E_{elstat} = -1.21$ kcal mol^{-1}, than to orbital and dispersion energies, $\Delta E_{pol} = -0.39$ kcal mol^{-1} and $\Delta E_{disp} = -0.23$ kcal mol^{-1}. For the *ag*-CEA → *gg*-CEA isomerization, both $\Delta E_{pol} = -1.25$ kcal mol^{-1} and $\Delta E_{disp} = -1.41$ kcal mol^{-1} energies are more

Table 7 Contribution of various energy terms to the total binding interactions between two $XH_2C^{\bullet}$ and $^{\bullet}CH_2NH_2$ radicals and to the *anti* → *gauche* energy change in 2-fluoroethylamine (FEA, X = F) and 2-chloroethylamine (CEA, X = Cl).[a] Values are in kcal mol^{-1}

Conformation	ΔE_{elstat}	ΔE_{ex+rep}	ΔE_{pol}	ΔE_{disp}	ΔE_{int}	ΔE_{prep}	ΔE
aa-FEA	−160.85	243.68	−159.29	−25.81	−102.27	11.49	−90.78
ag-FEA	−155.31	230.10	−155.91	−27.54	−108.66	17.74	−90.92
ga-FEA[b]	−163.56	246.11	−160.46	−25.87	−103.78	11.83	−91.95
gg-FEA[b]	−156.77	231.14	−157.53	−28.82	−111.98	19.67	−92.31
gg′-FEA	−154.09	231.18	−157.17	−28.23	−108.31	18.59	−89.72
aa-FEA → *ga*-FEA	−2.71	2.43	−1.17	−0.06	−1.51	0.34	−1.17
ag-FEA → *gg*-FEA	−1.46	1.04	−1.62	−1.28	−3.32	1.93	−1.39
ag′-FEA → *gg*′-FEA	1.22	1.08	−1.26	−0.69	0.35	0.84	1.19
aa-CEA	−159.58	243.59	−158.42	−29.51	−103.92	13.18	−90.74
ag-CEA	−154.10	230.80	−155.67	−31.34	−110.31	19.74	−90.57
ga-CEA[b]	−160.79	244.63	−158.81	−29.74	−104.71	13.39	−91.32
gg-CEA[b]	−154.99	231.76	−156.92	−32.75	−112.90	21.32	−91.58
gg′-CEA	−152.16	230.71	−156.07	−32.07	−109.59	20.46	−89.13
aa-CEA → *ga*-CEA	−1.21	1.04	−0.39	−0.23	−0.79	0.21	−0.58
ag-CEA → *gg*-CEA	−0.89	0.96	−1.25	−1.41	−2.59	1.58	−1.01
ag′-CEA → *gg*′-CEA	1.94	−0.09	−0.40	−0.73	0.72	0.72	1.44

[a] Labeling of various energy terms is the same as in Table 1. [b] Structure having an NH_2 hydrogen atom oriented toward a halogen atom.

Table 8 Energies (in kcal mol^{-1}) of vicinal hyperconjugative interactions in 2-fluoroethylamine (FEA, X = F) and 2-chloroethylamine (CEA, X = Cl) estimated from the second-order perturbative approach, $E(2)$ values, and deletion of the corresponding Fock matrix elements in the NBO basis, E(del). Calculated at the HF/6-311++G** level

	FEA					CEA				
	aa	*ag*	*ga*	*gg*	*gg′*	*aa*	*ag*	*ga*	*gg*	*gg′*
Vicinal hyperconjugation										
$E(2)_{\text{synclinal/anti}}$	20.02	20.03	23.11	22.80	22.79	22.04	22.25	24.98	24.85	24.66
$E(2)_{\text{synclinal/anti}}$ $a \rightarrow g$			3.09	2.77	2.76			2.94	2.60	2.41
$E(\text{del})_{\text{synclinal/anti}}$	18.84	18.85	21.36	21.04	21.06	20.86	20.95	22.90	22.73	22.62
$E(\text{del})_{\text{synclinal/anti}}$ $a \rightarrow g$			2.52	2.19	2.21			2.03	1.78	1.67
***Anti* hyperconjugation**										
C–H → C–H*	3.03	2.99	3.14	3.16	3.06	3.08	3.11	3.13	3.21	3.21
	3.03	2.99	3.38	3.14	3.23	3.08	3.07	3.71	3.42	3.56
	3.12	2.80				3.54	3.22			
	3.12	3.11				3.54	3.58			
C–X → C–N*	1.68	1.50				3.27	3.03			
C–N → C–X*	2.32	2.68				2.93	3.40			
C–H → C–X*			6.09	6.17	5.93			7.45	7.46	7.23
C–H → C–N*			4.92	4.06	4.43			4.91	4.02	4.24
C–X → C–H*			1.10	1.13	0.98			2.04	2.25	2.04
C–N → C–H*			1.03	1.26	1.08			1.11	1.46	1.29
Total $E(2)_{\text{anti}}$	16.30	16.07	19.66	18.92	18.71	19.44	19.41	22.35	21.82	21.57
Total $E(2)_{\text{anti}}$ $a \rightarrow g$			3.36	2.85	2.64			2.91	2.41	2.16

favourable than $\Delta E_{\text{elstat}} = -0.89$ kcal mol^{-1}. This compares with the situation in FEA, with the absolute values of ΔE_{elstat} and ΔE_{pol} being smaller and those of ΔE_{disp} larger relative to the corresponding values for FEA, which is in accord with the above discussion. In the case of the *ag′*-CEA → *gg′*-CEA rotation, the more favourable ΔE_{pol} and ΔE_{disp} energies are not large enough to override the 1.94 kcal mol^{-1} smaller electrostatic stabilization in *gg′ vs. ag′*, resulting in positive ΔE_{int} energy. This electrostatic destabilization is larger compared to the one in FEA (1.22 kcal mol^{-1}) which is due to the replacement of fluorine with chlorine atom. It is also larger than electrostatic destabilization following the *ag*-CE → *gg*-CE isomerization (0.59 kcal mol^{-1}, Table 3), which brings chlorine close to the oxygen lone pair, while the *aa*-CE → *ga*-CE rotation, also leading to the chlorine/oxygen lone pair interaction results in a more favourable $\Delta E_{\text{elstat}} = -1.29$ kcal mol^{-1}. The latter results could be attributed to the already mentioned observation that the more electronegative oxygen atom is more effective in electrostatic stabilization in *gauche* relative to the *anti* form, or its smaller destabilization. Interestingly, a change in the steric repulsion accompanying the *ag′*-CEA → *gg′*-CEA conformational isomerization is negligible (Table 7).

Among the orbital interactions, vicinal *anti* and total hyperconjugation do favour heavy atoms *gauche* arrangement more than the *anti*, but less so than in FEA (compare $a \rightarrow g$ values for FEA and CEA in Table 8). The C–H → C–Cl* and C–Cl → C–H* interactions are increased in *ga* and *gg* forms of CEA relative to the corresponding interactions in FEA by ∼1.3 kcal mol^{-1} and ∼1 kcal mol^{-1}, respectively, but concomitantly the C–Cl → C–N* and C–N → C–Cl* interactions become larger in *aa* and *ag* conformers of CEA by ∼1.6 kcal mol^{-1} and ∼0.6–0.7 kcal mol^{-1}, respectively, compared to the corresponding interactions in FEA. Together with somewhat smaller changes in other hyperconjugative interactions, the net result is less pronounced stereoelectronic stabilization for the *anti* → *gauche* isomerizations in the case of CEA.

The protonated forms of FEA and CEA, denoted herein as FEAH and CEAH, respectively, exist as one *gauche* and one *anti* conformer, which are energetically distinguishable (Fig. 5). The MP2/6-311++G** optimized structural parameters are given in Tables S9 and S10 in the ESI.† The FEAH shows a significant *gauche* effect of $\Delta E = -6.85$ kcal mol^{-1} (this work), which was earlier ascribed to a combination of intramolecular hydrogen bonding and stereoelectronic effects,[12e,13c] or electrostatic interactions.[10] Our data from energy decomposition analysis show that this *gauche* preference originates mostly from electrostatic energy term which is 2.7 times stronger than all orbital interaction stabilization (Table 9). It certainly involves C–F and N–H bond dipoles attraction, which are almost fully parallel ($\theta_{\text{FCNH}} = 0.2°$) and oppositely oriented. Contribution of ΔE_{disp} is small. The ΔE_{elstat} and ΔE_{pol} significantly overcome the steric repulsion, thus making the ΔE_{int} very favourable (−7.18 kcal mol^{-1}). It is just slightly diminished by the positive ΔE_{prep} energy. The existence of stereoelectronic *gauche* effect, too, is evident from stronger vicinal hyperconjugative interactions in *g*-FEAH with respect to *a*-FEAH, shown in Table 10. The most important contribution in the *gauche* form comes from the C–H → C–N* interaction which exceeds the C–H → C–F* one (5.3 kcal mol^{-1} and 3.9 kcal mol^{-1}, respectively). This contrasts their order in the free amine (Table 8) and is in accord with the relative order of the corresponding interactions in neutral and protonated alcohols.

Protonation of CEA increases the *gauche* preference from 0.6–1 kcal mol^{-1} in the free amine (Fig. 4 and Table 7) to

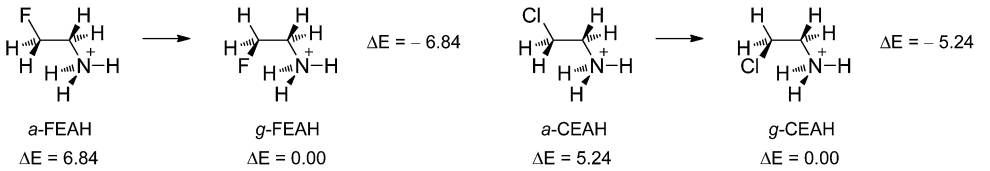

Fig. 5 Energy minimum conformations of protonated 2-fluoroethylamine (FEAH) and protonated 2-chloroethylamine (CEAH), their relative electronic energies (kcal mol^{-1}) and energy changes occurring upon *anti* → *gauche* rotation.

5.24 kcal mol^{-1} in CEAH (Fig. 5 and Table 9). Compared to CEA, the most important contributor to the increase in the *gauche* effect has to be attributed to the ΔE_{elstat} energy component, the stabilization of which increases from 0.9–1.2 kcal mol^{-1} in amine to 6.6 kcal mol^{-1} in its protonated form. In both compounds, favourable electrostatic energy also involves attraction between the almost antiparallel C–Cl and N–H dipoles, θ_{ClCNH} being 2.5°, 1.5° and 2.7° in *ga*-CEA, *gg*-CEA and *g*-CEAH, respectively. The second favourable energy contribution in CEAH comes from ΔE_{pol} energy term, which rises from 0.4–1.2 kcal mol^{-1} in amine to 2.3 kcal mol^{-1} in its protonated structure. Along with the ΔE_{disp}, these stabilizing interactions make the overall interaction energy favourable ($\Delta E_{int} = -5.43$ kcal mol^{-1}) by overcoming the increase in the steric repulsion. The ΔE_{int} is just slightly attenuated by the small positive ΔE_{prep} which amounts 0.19 kcal mol^{-1}. The charge transfer part of intramolecular hydrogen bond in *g*-CEAH (2.1 kcal mol^{-1}) is significantly smaller than in CEH (see above), while that in other *gauche* forms of (protonated) amines does not exceed 0.6 kcal mol^{-1}.

If the *gauche* effect in CEAH is compared to that in FEAH, it is smaller. This is mainly because of the decrease in the favourable electrostatic energy change ($\Delta E_{elstat} = -9.45$ kcal mol^{-1} for FEAH and $\Delta E_{elstat} = -6.65$ kcal mol^{-1} for CEAH), while the increase in the steric repulsion is smaller than that in FEAH (Table 9). The orbital interaction term is decreased, too, but less so than ΔE_{elstat}, while stabilizing contribution of dispersion forces become larger by 0.8 kcal mol^{-1}. The data in Table 10 reveal that the *a*-CEAH → *g*-CEAH isomerization benefits from stereoelectronic factors, as well, though less than the corresponding isomerization in FEAH. This should be attributed mainly to the increase in the C–Cl → C–N* interaction (5.3 kcal mol^{-1}) in *anti* conformer compared to the corresponding C–F → C–N* interaction (2.4 kcal mol^{-1}), which makes the overall stabilization energy change less favourable for chloro than for the fluoro derivative.

Comparison with NBO energy decomposition analysis

To be sure that conclusions of the work are not method-dependent, we also performed another energy decomposition analysis based on the NBO approach which treats a molecule as a single entity, that is it does not involve breaking of covalent bond. In the NBO energy decomposition analysis (NBOEDA), *anti* → *gauche* isomerization energy (ΔE) was decomposed into Lewis (ΔE_{Lewis}) and non-Lewis (ΔE_{deloc}) energy changes (eqn (3)), by using the NOSTAR keyword.[38] The Lewis energy corresponds to the energy of a hypothetical fully localized species, having all orbitals doubly occupied. The non-Lewis or delocalization energy represents all electron delocalization contributions to the conformational isomerization.

$$\Delta E = \Delta E_{Lewis} + \Delta E_{deloc} \quad (3)$$

The Lewis energy change comprises steric, electrostatic and structural effects. It was further decomposed into the steric (exchange repulsion) energy (ΔE_{steric}) and electrostatic-structural energy ($\Delta E_{elstat+struct}$) by using the STERIC keyword in the NBO analysis.[38] Thus, the overall conformational energy is partitioned into the three energy components (eqn (4) and Table S11 in the ESI†). Table S11† also contains the LMOEDA results for comparison.

$$\Delta E = \Delta E_{elstat+struct} + \Delta E_{steric} + \Delta E_{deloc} \quad (4)$$

The NBO energy decomposition has been applied to study the rotational barrier in ethane,[41] anomeric effect,[42] and conformational isomerization.[3c,43]

The NBOEDA results in Table S11† are qualitatively in agreement with the LMOEDA analysis, and they do not change conclusions of the work. These results support the finding that steric repulsion is smaller for chlorine derivatives, which is the result of structural changes taking place during the

Table 9 Contribution of various energy terms to the total binding interactions between two $XH_2C^{\bullet}$ and $^{\bullet}CH_2NH_3^+$ fragments and to the *anti* → *gauche* energy change in protonated 2-fluoroethylamine (FEAH, X = F) and protonated 2-chloroethylamine (CEAH, X = Cl).[a] Values are in kcal mol^{-1}

Conformation	ΔE_{elstat}	ΔE_{ex+rep}	ΔE_{pol}	ΔE_{disp}	ΔE_{int}	ΔE_{prep}	ΔE
a-FEAH	−131.03	202.24	−151.97	−29.64	−110.40	11.22	−99.18
g-FEAH	−140.48	208.20	−155.52	−29.78	−117.58	11.56	−106.02
a-FEAH → *g*-FEAH	−9.45	5.96	−3.55	−0.14	−7.18	0.34	−6.84
a-CEAH	−132.93	208.69	−156.12	−33.81	−114.17	13.40	−100.77
g-CEAH	−139.58	213.18	−158.46	−34.74	−119.60	13.58	−106.02
a-CEAH → *g*-CEAH	−6.65	4.49	−2.34	−0.93	−5.43	0.19	−5.24

[a] Labeling of various energy terms is the same as in Table 1.

Table 10 Energies (in kcal mol^{-1}) of vicinal hyperconjugative interactions in protonated 2-fluoroethylamine (FEAH, X = F) and protonated 2-choroethylamine (CEAH, X = Cl) estimated from the second-order perturbative approach, $E(2)$ values, and deletion of the corresponding Fock matrix elements in the NBO basis, E(del). Calculated at the HF/6-311++G** level

	a-FEAH	*g*-FEAH	*a*-CEAH	*g*-CEAH
Vicinal hyperconjugation				
$E(2)_{\text{synclinal/anti}}$	18.59	21.04	22.38	24.22
$E(2)_{\text{synclinal/anti}}$ $a \rightarrow g$		2.45		1.84
$E(\text{del})_{\text{synclinal/anti}}$	17.56	19.50	21.12	22.31
$E(\text{del})_{\text{synclinal/anti}}$ $a \rightarrow g$		1.94		1.20
***Anti* hyperconjugation**				
C–H → C–H*	2.88 (×2)	2.99	3.17 (×2)	3.08
	2.30 (×2)	2.50	2.79 (×2)	2.95
C–X → C–N*	2.42		5.26	
C–N → C–X*	1.43		1.98	
C–H → C–X*		3.97		5.21
C–H → C–N*		5.31		6.07
C–X → C–H*		1.23		2.51
C–N → C–H*		0.90		1.05
Total $E(2)_{\text{anti}}$	14.21	16.90	19.16	20.87
Total $E(2)_{\text{anti}}$ $a \rightarrow g$		2.69		1.71

conformational isomerization. The only exceptions to this observation are the *aa*-CEH → *ga*-CEH and *ag*-CEH → *gg*-CEH rotations, for which the LMOEDA also shows comparable results. In addition, in the NBOEDA analysis the negative $\Delta E_{\text{elstat+struct}}$ term means that *gauche* conformation is favoured by the sum of electrostatic and structural energies. The data in Table S11† show that this energy term is negative in all cases except for the *ag′*-CEH → *gg′*-CEH and *ag′*-CEA → *gg′*-CEA isomerizations, which could be ascribed to smaller electrostatic stabilization already observed for chlorine atom in the LMOEDA analysis.

Conclusions

In this paper, the origin of the *gauche* preference in 2-fluoroethanol, 2-chloroethanol, 2-fluoroethylamine, 2-chloroethylamine and their protonated forms, as well as the origin of *anti* preference in 1-chloro-2-fluoroethane are addressed from the standpoint of an energy decomposition analysis. In the case of (protonated) alcohols and amines, energies of *gauche* conformers were evaluated with respect to their corresponding *anti* conformers having the same conformational arrangement around the C–O and C–N bonds (*anti*, + *gauche* or − *gauche*). It has been found that the main factor leading to the *gauche* effect in alcohols, protonated alcohols and protonated amines is the electrostatic energy ΔE_{elstat}. Next come orbital interactions, involving pronounced charge transfer in hydrogen bonding only in the case of protonated 2-chloroethanol. In amines, the relative importance of ΔE_{elstat} and ΔE_{pol} depends on the type of conformational isomerization. Contribution of dispersion energy is usually the smallest one. The energies of these stabilizing interactions exceed the energy rise due to the increased Pauli repulsion in *gauche* forms. Structural changes occurring during the *anti* → *gauche* rotation of the heavy atom chain are energy consuming, but are overriden by the favourable interaction energy term. All gauche preferences also benefit from stereoelectronic effects, that is vicinal hyperconjugative interactions between XH_2C and CH_2Y fragments, except in the case of protonated 2-chloroethanol for which *aa*-CEH → *ga*-CEH and *ag*-CEH → *gg*-CEH isomerizations are not followed by an increase in the hyperconjugation.

Results from this work also show that electrostatic attractive interactions in *gauche* forms exceed those in *anti* forms even when our chemical intuition tells us that *gauche* conformers would suffer from dipolar and lone pair repulsion. This indicates that electrostatic interactions should better be considered as an all-charge phenomenon, because such partial interactions between bond dipoles or lone pairs cannot always account for the overall electrostatic energy change following conformational isomerization. In addition, electrostatic attraction in *gauche* forms relative to the *anti* ones is more important for more electronegative and smaller elements. That is, it decreases or even reverses its sign (becomes unfavourable contribution) when fluorine is substituted with chlorine, or when oxygen is substituted with nitrogen. In fact, *anti* preference in CFE and smaller *gauche* preference in chloro derivatives do not have their origin in the intuitively anticipated larger steric repulsion. They stem from a decrease in electrostatic stabilization upon going from *anti* to *gauche* structures, as well as a decrease in the orbital interaction energy. The former is often (somewhat) more pronounced. Or, if we still want to stick to some partial interactions, our results show that bringing smaller electronegative atoms close to each other results in nucleus–electron attraction overcoming the electron–electron and nucleus–nucleus repulsion. The relative magnitude of these attractive and repulsive interactions decreases, or even become reversed with increasing size and decreasing electronegativity of interacting atoms.

Our conclusions about the influence of atom size on the strength of electrostatic attraction related to *anti* → *gauche* conformational isomerization differ somewhat from conclusions from a very detailed analysis of chemical bonding in diatomic first and second octal row elements, which emphasized that electrons in more diffuse orbitals contribute more to the net electrostatic attraction, though orbital shape also has an influence.[34c]

Acknowledgements

This work was supported by the Ministry of Education, Science and Technological Development of the Republic of Serbia (Grant no. 172020).

References

1 D. O'Hagan, *Chem. Soc. Rev.*, 2008, **37**, 308–319.
2 E. L. Eliel, S. H. Wilen and L. N. Mander, in *Stereochemistry of Organic Compounds*, John Wiley & Sons, Inc., New York, 1994, pp. 606–615.

3 (*a*) P. R. Rablen, R. W. Hoffmann, D. A. Hrovat and W. Thatcher Borden, *J. Chem. Soc., Perkin Trans. 2*, 1999, 1719–1726; (*b*) B. M. Wong, M. M. Fadri and S. Raman, *J. Comput. Chem.*, 2008, **29**, 481–487; (*c*) F. R. Souza, M. P. Freitas and R. Rittner, *J. Mol. Struct.: THEOCHEM*, 2008, **863**, 137–140; (*d*) D. Nori-Shargh and J. E. Boggs, *Struct. Chem.*, 2011, **22**, 253–262.

4 S. Wolfe, *Acc. Chem. Res.*, 1972, **5**, 102–111.

5 K. B. Wiberg, M. A. Murcko, K. E. Laidig and P. J. MacDougall, *J. Phys. Chem.*, 1990, **94**, 6956–6959.

6 (*a*) L. Goodman, H. Gu and V. Pophristic, *J. Phys. Chem. A*, 2005, **109**, 1223–1229; (*b*) I. V. Alabugin, K. M. Gilmore and P. W. Peterson, *Wiley Interdiscip. Rev.: Comput. Mol. Sci.*, 2011, **1**, 109–141.

7 M. Baranac-Stojanović, *RSC Adv.*, 2014, **4**, 43834–43838.

8 C. R. S. Briggs, D. O'Hagan, H. S. Rzepa and A. M. Z. Slawin, *J. Fluorine Chem.*, 2004, **125**, 19–25.

9 D. O'Hagan, C. Bilton, J. A. K. Howard, L. Knight and D. J. Tozer, *J. Chem. Soc., Perkin Trans. 2*, 2000, 605–607.

10 D. Y. Buissonneaud, T. Van Mourik and D. O'Hagan, *Tetrahedron*, 2010, **66**, 2196–2202.

11 C. Sparr, E. Salamanova, W. B. Schweizer, H. M. Senn and R. Gilmour, *Chem.–Eur. J.*, 2011, **17**, 8850–8857.

12 (*a*) J. Huang and K. Hedberg, *J. Am. Chem. Soc.*, 1989, **111**, 6909–6913; (*b*) D. A. Dixon and B. E. Smart, *J. Phys. Chem.*, 1991, **95**, 1609–1612; (*c*) J. M. Bakke, L. H. Bjerkeseth, T. E. C. L. Rønnow and K. Steinsvoll, *J. Mol. Struct.*, 1994, **321**, 205–214; (*d*) C. Trindle, P. Crum and K. Douglass, *J. Phys. Chem. A*, 2003, **107**, 6236–6242; (*e*) C. R. S. Briggs, M. J. Allen, D. O'Hagan, D. J. Tozer, A. M. Z. Slawin, A. E. Goeta and J. A. K. Howard, *Org. Biomol. Chem.*, 2004, **2**, 732–740; (*f*) F. R. Souza and M. P. Freitas, *Comput. Theor. Chem.*, 2011, **964**, 155–159; (*g*) P. I. Nagy, *J. Phys. Chem. A*, 2013, **117**, 2812–2826; (*h*) R. A. Cormanich, R. Rittner, M. P. Freitas and M. Bühl, *Phys. Chem. Chem. Phys.*, 2014, **16**, 19212–19217.

13 (*a*) K.-M. Marstokk and H. Møllendal, *Acta Chem. Scand., Ser. A*, 1980, **34**, 15–29; (*b*) J. A. S. Smith and V. F. Kalasinsky, *Spectrochim. Acta, Part A*, 1986, **42**, 157–167; (*c*) I. Hyla-Kryspin, S. Grimme, S. Hruschka and G. Haufe, *Org. Biomol. Chem.*, 2008, **6**, 4167–4175; (*d*) J. R. Durig, A. Ganguly, C. Zheng, G. A. Gurigis, W. A. Herrebout, B. J. van der Veken and T. K. Gounev, *J. Mol. Struct.*, 2010, **968**, 36–47.

14 (*a*) J. A. K. Howard, V. J. Hoy, D. O'Hagan and G. T. Smith, *Tetrahedron*, 1996, **52**, 12613–12622; (*b*) J. D. Dunitz and R. Taylor, *Chem.–Eur. J.*, 1997, **3**, 89–98.

15 R. A. Cormanich, M. P. Freitas, C. F. Tormena and R. Rittner, *RSC Adv.*, 2012, **2**, 4169–4174.

16 (*a*) J. P. Snyder, N. S. Chandrakumar, H. Sato and D. C. Lankin, *J. Am. Chem. Soc.*, 2000, **122**, 544–545; (*b*) D. C. Lankin, G. L. Grunewald, F. A. Romero, I. Y. Oren and J. P. Snyder, *Org. Lett.*, 2002, **4**, 3557–3560; (*c*) A. Sun, D. C. Lankin, K. Hardcastle and J. P. Snyder, *Chem.–Eur. J.*, 2005, **11**, 1579–1591; (*d*) N. E. J. Gooseman, D. O'Hagan, A. M. Z. Slawin, A. M. Teale, D. J. Tozer and R. J. Young, *Chem. Commun.*, 2006, 3190–3192; (*e*) N. E. J. Gooseman, D. O'Hagan, M. J. G. Peach, A. M. Z. Slawin, D. J. Tozer and R. J. Young, *Angew. Chem., Int. Ed.*, 2007, **46**, 5904–5908.

17 (*a*) L. E. Zimmer, C. Sparr and R. Gilmour, *Angew. Chem., Int. Ed.*, 2011, **50**, 11860–11871; (*b*) E.-M. Tanzer, L. E. Zimmer, W. B. Schweizer and R. Gilmour, *Chem.–Eur. J.*, 2012, **18**, 11334–11342; (*c*) E.-M. Tanzer, W. B. Schweizer, M.-O. Ebert and R. Gilmour, *Chem.–Eur. J.*, 2012, **18**, 2006–2013; (*d*) Y. P. Rey, L. E. Zimmer, C. Sparr, E.-M. Tanzer, W. B. Schweizer, H. M. Senn, S. Lakhdar and R. Gilmour, *Eur. J. Org. Chem.*, 2014, 1202–1211.

18 (*a*) J. Huang and K. Hedberg, *J. Am. Chem. Soc.*, 1990, **112**, 2070–2075; (*b*) J. R. Durig, J. Liu and T. S. Little, *J. Phys. Chem.*, 1991, **95**, 4664–4672; (*c*) C. Cappelli, S. Corni and J. Tomasi, *J. Phys. Chem. A*, 2001, **105**, 10807–10815.

19 (*a*) A. Almenningen, L. Fernholt and K. Kveseth, *Acta Chem. Scand., Ser. A*, 1977, **31**, 297–305; (*b*) J. R. Durig, L. Zhou, T. K. Gounev, P. Klaeboe, G. A. Guirgis and L.-F. Wang, *J. Mol. Struct.*, 1996, **385**, 7–21; (*c*) S. X. Tian, N. Kishimoto and K. Ohno, *J. Phys. Chem. A*, 2003, **107**, 53–62.

20 H. Møllendal, S. Samdal and J.-C. Guillemin, *J. Phys. Chem. A*, 2011, **115**, 4334–4341.

21 A. Bondi, *J. Phys. Chem.*, 1964, **68**, 441–451.

22 C. Møller and M. S. Plesset, *Phys. Rev.*, 1934, **46**, 618–622.

23 M. J. Frisch, G. W. Trucks, H. B. Schlegel, G. E. Scuseria, M. A. Robb, J. R. Cheeseman, G. Scalmani, V. Barone, B. Mennucci, G. A. Petersson, H. Nakatsuji, M. Caricato, X. Li, H. P. Hratchian, A. F. Izmaylov, J. Bloino, G. Zheng, J. L. Sonnenberg, M. Hada, M. Ehara, K. Toyota, R. Fukuda, J. Hasegawa, M. Ishida, T. Nakajima, Y. Honda, O. Kitao, H. Nakai, T. Vreven, J. A. Montgomery Jr, J. E. Peralta, F. Ogliaro, M. Bearpark, J. J. Heyd, E. Brothers, K. N. Kudin, V. N. Staroverov, T. Keith, R. Kobayashi, J. Normand, K. Raghavachari, A. Rendell, J. C. Burant, S. S. Iyengar, J. Tomasi, M. Cossi, N. Rega, J. M. Millam, M. Klene, J. E. Knox, J. B. Cross, V. Bakken, C. Adamo, J. Jaramillo, R. Gomperts, R. E. Stratmann, O. Yazyev, A. J. Austin, R. Cammi, C. Pomelli, J. W. Ochterski, R. L. Martin, K. Morokuma, V. G. Zakrzewski, G. A. Voth, P. Salvador, J. J. Dannenberg, S. Dapprich, A. D. Daniels, O. Farkas, J. B. Foresman, J. V. Ortiz, J. Cioslowski and D. J. Fox, *Gaussian 09 (Revision D.01)*, Gaussian, Inc., Wallingford CT, 2013.

24 P. Su and H. Li, *J. Chem. Phys.*, 2009, **131**, 014102.

25 M. W. Schmidt, K. K. Baldridge, J. A. Boatz, S. T. Elbert, M. S. Gordon, J. H. Jensen, S. Koseki, N. Matsunaga, K. A. Nguyen, S. J. Su, T. L. Windus, M. Dupuis and J. A. Montgomery Jr, *J. Comput. Chem.*, 1993, **14**, 1347–1363, Gamess (2013-R1 version) was used.

26 (*a*) K. Kitaura and K. Morokuma, *Int. J. Quantum Chem.*, 1976, **10**, 325–340; (*b*) K. Morokuma, *Acc. Chem. Res.*, 1977, **10**, 294–300.

27 G. te Velde, F. M. Bickelhaupt, E. J. Baerends, C. Fronseca Guerra, S. J. A. Van Gisbergen, J. G. Snijders and T. Ziegler, *J. Comput. Chem.*, 2001, **22**, 931–967.

28 F. M. Bickelhaupt and E. J. Baerends, *Angew. Chem., Int. Ed.*, 2003, **42**, 4183–4188.

29 A. Szabó, A. Kovács and G. Frenking, *Z. Anorg. Allg. Chem.*, 2005, **631**, 1803–1809.
30 H. Jacobsen and T. Ziegler, *J. Am. Chem. Soc.*, 1994, **116**, 3667–3679.
31 (*a*) M. El-Hamdi, W. Tiznado, J. Poater and M. Solà, *J. Org. Chem.*, 2011, **76**, 8913–8921; (*b*) M. Baranac-Stojanović, *Chem.–Eur. J.*, 2014, **20**, 16558–16565.
32 J. Poater, R. Visser, M. Solà and F. M. Bickelhaupt, *J. Org. Chem.*, 2007, **72**, 1134–1142.
33 (*a*) D. Cappel, S. Tüllmann, A. Krapp and G. Frenking, *Angew. Chem., Int. Ed.*, 2005, **44**, 3617–3620; (*b*) I. Fernández and G. Frenking, *Chem.–Eur. J.*, 2006, **12**, 3617–3629; (*c*) I. Fernández and G. Frenking, *Faraday Discuss.*, 2007, **135**, 403–421.
34 (*a*) C. Esterhuysen and G. Frenking, *Theor. Chem. Acc.*, 2004, **111**, 381–389; (*b*) A. Kovács, C. Esterhuysen and G. Frenking, *Chem.–Eur. J.*, 2005, **11**, 1813–1825; (*c*) A. Krapp, F. M. Bickelhaupt and G. Frenking, *Chem.–Eur. J.*, 2006, **12**, 9196–9216.
35 E. D. Glendening, J. K. Badenhoop, A. E. Reed, J. E. Carpenter, J. A. Bohmann, C. M. Morales, C. R. Landis and F. Weinhold, *NBO 6.0*, Theoretical Chemistry Institute, University of Wisconsin, Madison, WI, 2013.
36 N. C. Craig, A. Chen, K. Hwan Suh, S. Klee, G. C. Mellau, B. P. Winnewisser and M. Winnewisser, *J. Am. Chem. Soc.*, 1997, **119**, 4789–4790.
37 H. Takeo, C. Matsumura and Y. Morino, *J. Chem. Phys.*, 1986, **84**, 4205–4210.
38 For details, see: (*a*) E. D. Glendening, C. R. Landis and F. Weinhold, *Wiley Interdiscip. Rev.: Comput. Mol. Sci.*, 2012, **2**, 1–42; (*b*) F. Weinhold and C. R. Landis, in *Discovering Chemistry with Natural Bond Orbitals*, John Wiley & Sons, Inc., 2012; (*c*) F. Weinhold, *NBO Manual*, Board of Regents of the University of Wisconsin System on behalf of the Theoretical Chemistry Institute, 1996–2008.
39 H.-W. Xi, M. Karni and Y. Apeloig, *J. Phys. Chem. A*, 2008, **112**, 13066–13079.
40 (*a*) Y. Mo, W. Wu, L. Song, M. Lin, Q. Zhang and J. Gao, *Angew. Chem., Int. Ed.*, 2004, **43**, 1986–1990; (*b*) Y. Mo and J. Gao, *Acc. Chem. Res.*, 2007, **40**, 113–119.
41 L. Goodman, H. Gu and V. Pophristic, *J. Chem. Phys.*, 1999, **110**, 4268–4274.
42 M. P. Freitas, *Org. Biomol. Chem.*, 2013, **11**, 2885–2890.
43 (*a*) L. A. F. Andrade, J. M. Silla, C. J. Duarte, R. Rittner and M. P. Freitas, *Org. Biomol. Chem.*, 2013, **11**, 6766–6771; (*b*) K. M. S. Gonçalves, D. R. Garcia, T. C. Ramalho, J. D. Figueroa-Villar and M. P. Freitas, *J. Phys. Chem. A*, 2013, **117**, 10980–10984.